Beamforming for Optimization of Throughput in 5G Networks - Assignment 3

Sun Haoxin, Wu Yujie, Xu Zewei
School of Computer and Communication Sciences, EPFL, Switzerland

***Abstract*—This report presents our results in throughput optimization by beamforming for 5G networks. In this project, we exploit 2 different beamforming algorithms, i.e., matched beamforming and *flexibeam*, to align the main lobe of the base station to users. We first display how to derive the theoretical expression for beamforming weights in these two methods, and how to estimate the direction of arrival (DOA) of signals from real data. Then both these algorithms are tested with simulated data to evaluate their performance. Evaluations on real data are also performed to check if they are still efficient in real applications. From our numerical results, matched beamforming performs well when users are dense and DOA estimation is accurate, but these conditions may not be satisfied in real scenarios. The *flexibeam* algorithm is suitable in applications when there are a large number of antennas on the base station and the antenna array is in specific geometry. It outperforms matched beamforming when users lie in a scattered pattern or estimation of DOA is not accurate, implying its effectiveness in real applications.**

I. Introduction

In recent years, 4G communication systems are not capable of handling the increasing number of end devices and requirements for higher data rates and lower latency. Thus, in the latest generation of communications, 5G, techniques like millimeter wave and massive MIMO are introduced [1]. However, mmWave suffers from large loss and short transmission distance compared with low-frequency signals. Beamforming is a key technique to overcome these problems as it can aggregate the energy of the antenna array in particular directions while suppressing propagation energy in others. Different algorithms related to beamforming are proposed by researchers, like hybrid beamforming [2], smart antennas [3] and so on.

In the project, we try to implement two different beamforming methods, namely matched beamforming and *flexibeam* [4], [5] to achieve high average throughput among user equipment (UE). As in real scenarios, conditions like the wireless network infrastructure, user behavior vary a lot, apart from their performance on the average throughput, we also need to consider these techniques' constraints and limitations so that the best method can be chosen given a specific application scenario.

This report is organized as follows. Section II displays the system models and theoretical calculation of both beamforming methods, Section III shows numerical results of these algorithms with simulated data and real datasets, as well as our analysis based on these results. Finally, Section IV concludes our project and Section V shows possible work directions in the future.

II. Materials and Methods

In this section, we first demonstrate the model we use in this project, then display how to derive the mathematical expressions of these algorithms respectively and how to estimate the direction of arrival from real data.

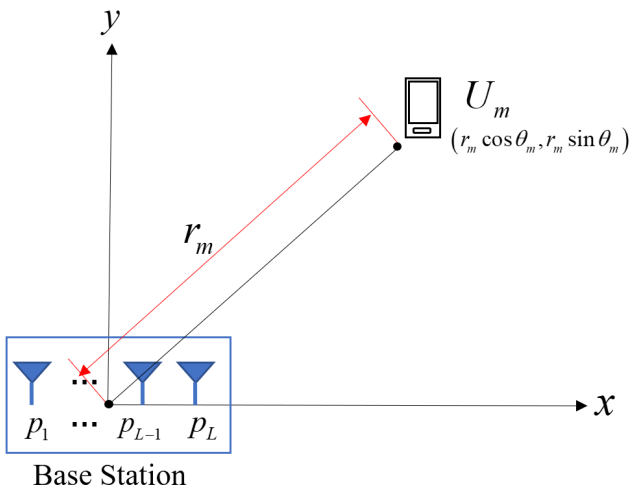

Figure 1. The system block diagram.

A. System models for beamforming

We consider a 2D downlink MISO cellular system as shown in Fig. 1. In this system, there is one base station (BS) with L omni-directional antennas deployed on it, at position $\boldsymbol{p_i}$. Each antenna L_i has a beamforming weight b_i, i.e., the gain and phase delay are $\gamma_i = |b_i|$ and $\phi_i = arg(b_i)$ respectively. Assume each antenna has the same input baseband signal $s(t)$, then we can derive the signal $x_i(t)$. In other words, the emitted signal of L_i is:

$$x_i(t) = b_i s(t) = \gamma_i e^{j\phi_i} s(t),\ \forall i = 1, 2, ..., L. \qquad (1)$$

A mobile user U_m, which is currently at position $\boldsymbol{r_m} = (r_m \cos\theta_m, r_m \sin\theta_m)$, is moving in this area and connects to this base station. Assume U_m lies in the far field, i.e., far away from the BS, then neglecting channel fading, the signal $y(t)$ received by U_m is a linear sum of the emitted

signals with different phase delays:

$$y(t) = s_o(t) \sum_{i=1}^{L} \gamma_i e^{j\phi_i} e^{-j2\pi \frac{<\boldsymbol{p_i}, \boldsymbol{r_m}>}{r_m \lambda}}, \quad (2)$$

where $\lambda \in \mathbb{R}_+$ denotes the wavelength of $s(t)$, and $s_o(t)$ is the received signal from the antenna located at the origin, which is only a reference for calculation and can be virtual. Equivalently, Eq. 2 can be expressed by the DOA θ_m:

$$y(t) = s_o(t) \sum_{i=1}^{L} \gamma_i e^{j\phi_i} e^{-j2\pi \frac{<\boldsymbol{p_i}, (\cos\theta_m, \sin\theta_m)>}{\lambda}}. \quad (3)$$

B. Matched beamforming

The calculation of matched beamforming weights is intuitive. From Eq. 2, we know that the equivalent channel gain is the norm of the complex summation. Thus, the design goal is to maximize this norm. Considering the triangle inequality, when the user U_m receives each signal with a zero phase, i.e., $y_i(t)$ is a real number, the received channel gain will be maximized. Without loss of generality, we assume each antenna's transmitting power is the same. Then, given the UE's position $\boldsymbol{r_m}$, each antenna's beamforming weight b_i can be computed by the following equation:

$$b_i = \gamma_i e^{j\phi_i} = \frac{1}{\sqrt{L}} e^{j2\pi \frac{<\boldsymbol{p_i}, \boldsymbol{r_m}>}{r_m \lambda}}, \ \forall i = 1, 2, ..., L. \quad (4)$$

The coefficient $\frac{1}{\sqrt{L}}$ is used to normalize the transmitting power of the base station. An equivalent expression corresponding to Eq. 3 can also be derived:

$$b_i = \frac{1}{\sqrt{L}} e^{j2\pi \frac{<\boldsymbol{p_i}, (\cos\theta, \sin\theta)>}{\lambda}}, \ \forall i = 1, 2, ..., L. \quad (5)$$

In other words, each antenna will include a phase shift to compensate for the phase delay caused by the distance between the UE and itself.

It can be noticed that matched beamforming generates high-power waves only in the steering direction. Since the RF-spectrum is a shared medium while multiple users are connecting to the BS simultaneously, for matched beamforming, we assume it is a time-division multiple access (TDMA) channel, allowing several users to share the same frequency channel by dividing the signal into different time slots. Assume there are K users in the area and their movement can be neglected for one second. Generally, the system model is demonstrated as follows.

1) At the beginning of every second, the base station detects the positions of users and gets M directions $(\theta_1, \theta_2, ..., \theta_M)$ where users are located.
2) Equally divide 1s into M slots $(t_1, t_2, ..., t_M)$. After every $1/M$ s, direction of beamforming is changed. For example, the beamformed direction at slot t_m equals θ_m.
3) In t_m slots, all users share the same channel in a TDMA manner. So we can also equally divide t_m into K parts. Define the k^{th} time slot in slot t_m as t_{mk}, then $t_{mk} = 1/MK$ s is allocated to user k. This means the users transmit in rapid succession within their own timeslots.

The slot model is shown in Fig. 2.

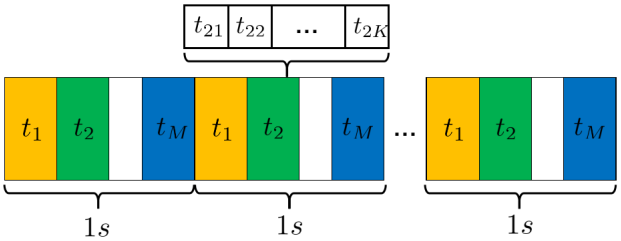

Figure 2. Slot model based on TDMA.

C. Flexibeam

Indeed, matched beamforming is a low-complexity algorithm as it only needs to calculate each antenna's phase delay. However, in real scenarios in 5G, multiple users are communicating with one base station from different DOAs, but matched beamforming can only form a narrow main lobe to cover a small area. When users are not in dense, this leads to really low channel gains to users not close to the currently serving one, resulting in bad quality of service and low average throughput. To overcome this disadvantage, we derive an improved beamforming algorithm named *flexibeam* which can generate a wider main lobe and cover a larger range of users.

Assume there are infinite and continuous transmitting antennas in the 2D plane, we use the symbol $x(t, \boldsymbol{p})$ to denote the emitted signal of the antenna located at $\boldsymbol{p}$. Based on Eq. 1, $x(t, \boldsymbol{p})$ can be written as:

$$x(t, \boldsymbol{p}) = \gamma(\boldsymbol{p}) e^{j\phi(\boldsymbol{p})} s(t) = \omega^*(\boldsymbol{p}) s(t), \ \boldsymbol{p} \in \mathbb{R}^2, \quad (6)$$

where $\omega^*(\boldsymbol{p})$ is our desired beamforming weight for this antenna. Under this assumption, the received signal of a user at position $\boldsymbol{r} = r(\cos\theta, \sin\theta)$ can be extended from Eq. 2:

$$\begin{aligned} y(t) &= s_o(t) \left(\int_{\mathbb{R}^2} \omega^*(\boldsymbol{p}) e^{-j2\pi \frac{<\boldsymbol{p}, \boldsymbol{r}>}{r\lambda}} d\boldsymbol{p} \right) \\ &= s_o(t) \hat{\omega}^*(\boldsymbol{r}), \ \boldsymbol{r} \in \mathbb{R}^2. \end{aligned} \quad (7)$$

Therefore, now the radiation pattern is the amplitude of $\hat{\omega}(\boldsymbol{r})$, which in fact acts as a spatial filter. From Eq. 7 we know that $\omega(\boldsymbol{p})$ and $\hat{\omega}(\boldsymbol{r})$ are related, and their relationship can be described as:

$$\hat{\omega}(\boldsymbol{r}) = \int_{\mathbb{R}^2} \omega(\boldsymbol{p}) e^{j2\pi \frac{<\boldsymbol{p}, \boldsymbol{r}>}{r\lambda}} d\boldsymbol{p}, \ \boldsymbol{r}, \ \boldsymbol{p} \in \mathbb{R}^2. \quad (8)$$

The format of Eq. 8 implies that $\omega(\boldsymbol{p})$ and $\hat{\omega}(r\lambda\boldsymbol{r})$ are actually a couple of 2D Fourier Transform. Therefore, getting one of them will lead to the clear expression of the other.

Given any desired radiation pattern $\hat{\omega}(\boldsymbol{r})$, we can numerically calculate the beamforming weight $\omega(\boldsymbol{p})$. However, $\hat{\omega}(\boldsymbol{r})$ can also be carefully designed so that the closed-form expression of $\omega(\boldsymbol{p})$ is easy to derive. Here we use a 2D Gaussian distribution to model the desired radiation pattern, and $\hat{\omega}(\boldsymbol{r})$ can be expressed as:

$$\begin{aligned} \hat{\omega}(\boldsymbol{r}) &= \frac{1}{2\pi\sigma^2} e^{-\frac{\|\boldsymbol{r}-\boldsymbol{r_0}\|^2}{2\sigma^2}}, \\ \sigma &= r\sigma_\theta = r\sqrt{2-2\cos\Theta}, \end{aligned} \tag{9}$$

where $\boldsymbol{r_0} = r(\cos\theta_0, \sin\theta_0)$ is the mean position of all users, and $\Theta \in [0, 180^\circ]$ is the desired beamwidth, indicating user density. Obviously, the bigger Θ is, the more scattered users are, and the wider main lobe is required. Then using 2D Fourier Transform and its scaling property, we can easily compute the beamforming weight $\omega_0(\boldsymbol{p})$ for the antenna located at $\boldsymbol{p}$:

$$\begin{aligned} \omega_0(\boldsymbol{p}) =& \frac{1}{r\lambda}(2\pi)^2 e^{-\frac{2\pi^2\sigma^2\|\boldsymbol{p}\|^2}{(r\lambda)^2}} e^{-j2\pi\frac{<\boldsymbol{p},\boldsymbol{r_0}>}{r\lambda}} \\ =& \alpha e^{-\frac{2\pi^2\sigma_\theta^2\|\boldsymbol{p}\|^2}{\lambda^2}} e^{-j2\pi\frac{<\boldsymbol{p},(\cos\theta_0,\sin\theta_0)>}{\lambda}}, \end{aligned} \tag{10}$$

where α is a constant and only affects transmitting power.

In real applications, the BS only have L antennas, and L is finite. Thus, the continuous function $\omega(\boldsymbol{p})$ boils down to discrete $\omega(\boldsymbol{p_i})$ by sampling the original function at specific antennas' positions $\boldsymbol{p_i}$. Besides, to keep the transmitting power of the base station remain the same with different infrastructures, we do normalization on the amplitude of each beamforming weight to get the desired $\omega(\boldsymbol{p_i})$:

$$\begin{aligned} \omega_0(\boldsymbol{p_i}) &= \alpha e^{-\frac{2\pi^2\sigma_\theta^2\|\boldsymbol{p_i}\|^2}{\lambda^2}} e^{-j2\pi\frac{<\boldsymbol{p_i},(\cos\theta_0,\sin\theta_0)>}{\lambda}}, \\ \omega(\boldsymbol{p_i}) &= \frac{\omega_0(\boldsymbol{p_i})}{\sqrt{\sum_{i=1}^{L}\|\omega_0(\boldsymbol{p_i})\|^2}},\ i = 1, 2, ..., L. \end{aligned} \tag{11}$$

By introducing the desired beamwidth Θ, *flexibeam* can calculate beamforming weights via Eq. 11, so that the generated main lobe can cover a large area. But it should also be noticed that compared with matched beamforming weights, the only difference is amplitudes (phase delays are the same), which are affected by the distance of antennas away from the origin. In other words, *flexibeam* is effective only when antennas on the BS have different distances from the origin.

D. Another way to derive flexibeam's expression

In this paragraph, we would like to show another way to derive the expression of *flexibeam*. For simplicity, we assume that the position of user $\boldsymbol{r}$ is situated on the unit circle, so $\boldsymbol{r} = (\cos\theta, \sin\theta)$ and the wavelength $\lambda = 1$. So Eq. 7 can be written as

$$\begin{aligned} y(t) &= s_o(t)\left(\int_{\mathbb{R}^2} \omega^*(\boldsymbol{p}) e^{-j2\pi<\boldsymbol{p},\boldsymbol{r}>} d\boldsymbol{p}\right) \\ &= s_o(t)\hat{\omega}^*(\boldsymbol{r}),\ \boldsymbol{r} \in \mathbb{R}^2, \end{aligned} \tag{12}$$

and the same reasoning goes for Eq. 8:

$$\hat{\omega}(\boldsymbol{r}) = \int_{\mathbb{R}^2} \omega(\boldsymbol{p}) e^{j2\pi<\boldsymbol{p},\boldsymbol{r}>} d\boldsymbol{p}. \tag{13}$$

Once we obtain $\hat{\omega}(\boldsymbol{r})$, we can compute $\omega(\boldsymbol{p})$ through the following formula:

$$\omega(\boldsymbol{p}) = \int_{\mathbb{R}^2} \hat{\omega}(\boldsymbol{r}) e^{-j2\pi<\boldsymbol{p},\boldsymbol{r}>} d\boldsymbol{r}. \tag{14}$$

Using the Gaussian distribution defined in Eq. 9, $\omega(\boldsymbol{p})$ can be written as below:

$$\omega(\boldsymbol{p}) = (2\pi)^n e^{-2\pi^2\sigma^2||\boldsymbol{p}||^2} e^{-j2\pi<\boldsymbol{p},\boldsymbol{r}_0>}. \tag{15}$$

When $\lambda \neq 1$, we can replace $\boldsymbol{p}$ by $\boldsymbol{p}/\lambda$ in Eq. 15, i.e., normalizing the vector so that it gets back to the $\lambda = 1$ case. It can be clearly seen that after doing normalization on transmitting power $\sum_{i=1}^{L}\|\omega_0(\boldsymbol{p_i})\|^2$, Eq. 15 is the same as Eq. 11 by using $\boldsymbol{p}/\lambda$.

Therefore, rather than using the scaling property of 2D Fourier Transform, here we normalize the variables by the wavelength and as a result get the same expression as the previous part.

E. Flexibeam for multi-cluster users

When user density cannot be simply modeled by only one Gaussian distribution (e.g. there are multiple separate clusters of users), rather than using TDMA like in matched beamforming, which leads to degradation of average throughput, we can form several main lobes by using the sum of several Gaussian distributions to model the density and then applying *flexibeam*. Assuming there are J clusters of users (the BS receives signals from J different directions), now the desired radiation pattern can be expressed as:

$$\begin{aligned} \hat{\omega}(\boldsymbol{r}) &= \sum_{j=1}^{J}\hat{\omega}_j(\boldsymbol{r}) = \sum_{j=1}^{J}\frac{1}{2\pi\sigma_j^2} e^{-\frac{\|\boldsymbol{r}-\boldsymbol{r_{0j}}\|^2}{2\sigma_j^2}}, \\ \sigma_j &= r\sigma_{\theta j} = r\sqrt{2-2\cos\Theta_j},\ j = 1, 2, ...J. \end{aligned} \tag{16}$$

In Eq. 16, we can use J Gaussian distributions $\hat{\omega}_j(\boldsymbol{r})$ with different means $\boldsymbol{r_{0j}}$ and variances σ_j^2 to describe it. In the DOA estimation, the mean of each distribution $\boldsymbol{r_{0j}}$ can be derived by finding all peak values in the received spatial power spectrum, with J the number of peak values. The variance σ_j^2 of each distribution can be obtained by calculating the peak width.

An alternative way to model these users is to use the Gaussian Mixture Model, which can also provide the number of clusters, the mean value and the variance of each cluster by applying maximum likelihood estimation.

Then from previous parts, we know that via Eq. 11 each $\hat{\omega}_j(\boldsymbol{r})$ corresponds to its own $\omega_j(\boldsymbol{p_i})$. Due to Fourier

Transform's linearity, the resulting $\omega(\boldsymbol{p_i})$ is a normalized sum of these individual results:

$$\omega(\boldsymbol{p_i}) = \frac{1}{\sqrt{J}} \sum_{j=1}^{J} \omega_j(\boldsymbol{p_i}),\ i = 1, 2, ..., L. \tag{17}$$

By doing this, rather than having only one main lobe and suppressing transmitting power in all others, the transmitted signal generated by *flexibeam* can now have multiple lobes pointing to different directions with relatively high power.

F. Data rate and throughput

We assume the channel between the BS and users is an additive white Gaussian noise (AWGN) channel. Then, if we denote the white noise variance by σ^2, the data rate of a user can be derived according to Shannon's capacity theorem:

$$r = B \log_2 \left(1 + C_0 \frac{\|y(t)\|^2}{\sigma^2}\right), \tag{18}$$

where B denotes the channel bandwidth allocated to this user, $C_0 < 1$ is a constant that denotes the gap between the channel capacity and the achieved data rate due to factors like imperfect channel coding.

G. Direction of arrival

Direction of arrival (DOA) is the angle of propagation from space center to user. Assume DOA estimation is in 2D-space and the antenna is located uniformly in a circular array. As mentioned in Part A, UE's position $\boldsymbol{r_m} = (r_m \cos\theta_m, r_m \sin\theta_m)$. L is the number of antenna, coordinates of antenna i is $\boldsymbol{p_i} = (x_i, y_i)^{\mathrm{T}}$ where $i = 1, 2, ..., L$. The geometry of antenna and user is shown in Fig. 3. $s(t)$ is

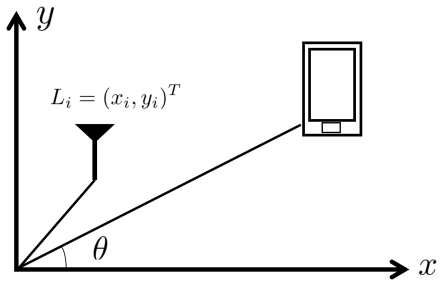

Figure 3. Geometry of the antenna and the user.

the input baseband signal, λ is the emitted wavelength and $k = 2\pi/\lambda$. $a(\theta)$ is the antenna propagation vector.

$$a(\theta) = g(\theta)[e^{-jk\langle \boldsymbol{p_1}, b(\theta)\rangle}\ e^{-jk\langle \boldsymbol{p_2}, b(\theta)\rangle}\ ...\ e^{-jk\langle \boldsymbol{p_L}, b(\theta)\rangle}]^{\mathrm{T}}, \tag{19}$$

where g(θ) is the gain matrix for antenna 1 to L. For a uniform circle antenna array, the antennas' position is $\boldsymbol{p_i} = R(\cos(\frac{2\pi(i-1)}{L}), \sin(\frac{2\pi(i-1)}{L}))$ and $b(\theta) = (\cos(\theta), \sin(\theta))^{\mathrm{T}}$.

If there are M signals impinge on the L-dimensional antenna from DOAs $\theta_1, ..., \theta_M$, the field $f(t)$ measured with added noise $n(t)$ can be written as

$$f(t) = \sum_{m=1}^{M} a(\theta_m) s_m(t) + n_m(t),\ l = 1,\ 2,\ ...,\ L. \tag{20}$$

Assume we have the cross-variance information among users. The spatial covariance matrix is calculated as Eq. 21.

$$R = E\{f(t) f^{\mathrm{H}}(t)\}. \tag{21}$$

DOA finds propagation direction by identifying the direction having maximum power P. In the real world, users distribute randomly in an area. Users would possibly gather in some directions. In this case, it is difficult to distinguish between the clusters of users which are close to each other. Besides, the number of users could be much greater than the number of antennas. Furthermore, we do not know the accurate position of users. Since the number of antennas is smaller than the number of users, to get an accurate propagation angle, Capon's beamforming is utilized [6]. Capon's beamformer minimizes the power contributed by noise and any signals coming from a direction other than θ, increasing resolution between angles. Capon beamformer's spatial spectrum is calculated as

$$P_{CAP}(\theta) = \frac{1}{a^{\mathrm{H}}(\theta) \hat{R}^{-1} a(\theta)}. \tag{22}$$

After obtaining the power distribution in $(0, 2\pi)$, the positions of users are θs which have local maximum power.

III. Results

Based on the derived beamforming weights' expression, in this section, we do numerical tests and display the results of these two beamforming algorithms respectively. We first do the calculation with simulated data, then two real datasets are considered.

A. Results with simulation data

To facilitate the explanation of theory and evaluate the algorithm's performance, we implement matched beamforming and *flexibeam* on simulated data respectively.

We first measure the influence of antennas' number. We assume the base station deploys a uniform circular antenna array with radius $\frac{\lambda}{2}$, and the mobile user is centered at direction $40°$. Simulation parameters are listed in Table I. Then we plot the radiation patterns of matched beamforming and *flexibeam* with the different number of antennas, as shown in Fig. 4 and Fig. 5 respectively. As we discussed in the previous section, when there is only one DOA and all antennas lie in a circle, *flexibeam* boils down to matched beamforming so that Fig. 4 and Fig. 5 are the same. Obviously, when the density of antennas is large, signals transmit to a broader area with greater strength, as more antennas always lead to better beamforming performance.

Table I
VALUE SETTINGS OF SIMULATION PARAMETERS

Parameter	Value
Wave length λ	1 m
Power of $s(t)$	0.1 W
Desired beamwidth Θ	20°
Bandwidth B	2 MHz
Variance of white noise σ^2	0.1
Constant C_0	0.8

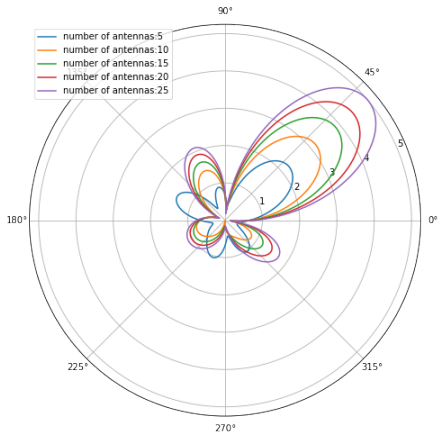

Figure 4. Matched beamforming with different number of antennas.

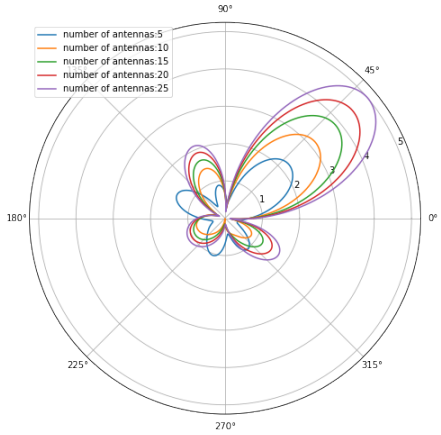

Figure 5. *Flexibeam* with different number of antennas.

The radius of the antennas' position is another important parameter. We assume antennas on the base station have a concentric circle geometry structure. 20 antennas uniformly distribute on one circle and the i^{th} circle has a radius of $\frac{\lambda}{i+1}$. Then the radiation graphs of four different structures are plotted in Fig. 6 and Fig. 7. Since now antennas lie on circles with different radii, *flexibeam* would form different patterns from those of matched beamforming. Indeed, Fig. 6 and Fig. 7 indicate that *flexibeam* generates wider main lobes, and 4 layers of antennas enjoy the widest radiation area and greatest signal strength.

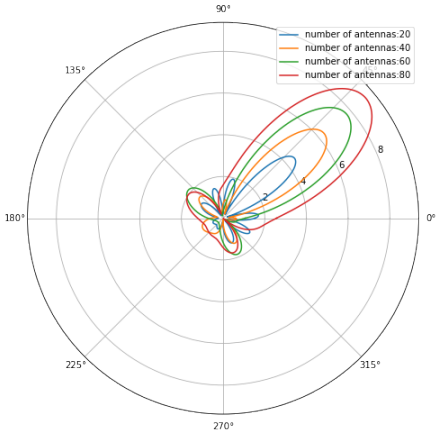

Figure 6. Matched beamforming with different number of antennas and different radius.

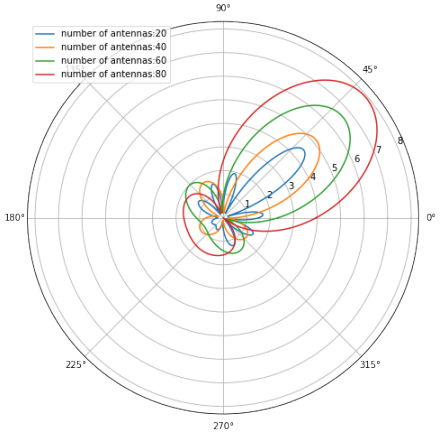

Figure 7. *Flexibeam* with different number of antennas and different radius.

As demonstrated in the previous section, *flexibeam* uses a 2D Gaussian distribution to model its desired radiation

pattern, aiming to cover more users who are close to the mean position ($\boldsymbol{r_0}$). For a fixed number of antennas, we evaluate the radiation pattern under different Θ under the condition that there are 15 antennas on each concentric circle and the circles' radius are 0.2λ, 0.5λ, λ and 1.5λ respectively. According to Fig. 8, the beamwidth of the main

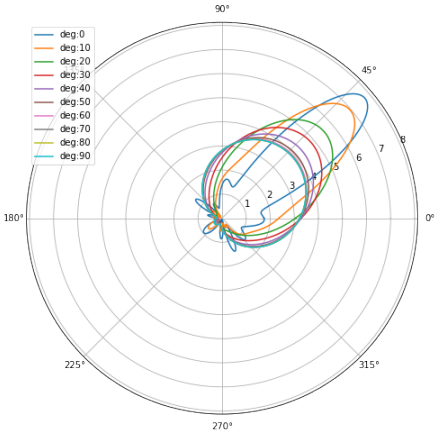

Figure 8. *Flexibeam* with different Θ.

lobe increases as Θ grows, which meets our expectations. However, the increment decreases as Θ becomes large because, in terms of large Θ, the beam shape struggles to cover the whole range while balancing it with less energy for each direction.

Finally, we analyze *flexibeam*'s capacity to point to several directions simultaneously. Suppose there are two clusters of users who are in direction $r_{0,1} = 0°$ and $r_{0,2} = i \times 20°$, where $i = 0, 1, 2, 3, 4$. Under the condition that 20 antennas are separately distributed in 3-layer concentric circles (radius 0.5λ, λ, and 1.5λ), the radiation pattern is shown in Fig. 9. This figure proves that *flexibeam* can point in several directions with high power at the same time. However, if the two directions are too close, the middle region between these two would have higher channel gain than any of them because the distributions overlap.

In order to quantify the performance of *flexibeam*, we calculate the data rate in these simulations. To model user distribution, von-Mises distribution is applied here. We generate two clusters of users with concentration factor and measure of location equal to $4, 2.6$ and $2, 4.5$ respectively. The plot of user distribution is in Fig. 10. Besides, we set the antenna structure to be 3-layer concentric circles with antenna numbers 10, 30, 50 and radius 0.1λ, 0.5λ, λ respectively. Under these conditions, following the assumption of the AWGN channel model in the previous section, matched beamforming has an average data rate of 8.31×10^4 bps while *flexibeam* has 1.34×10^5 bps. This implies the

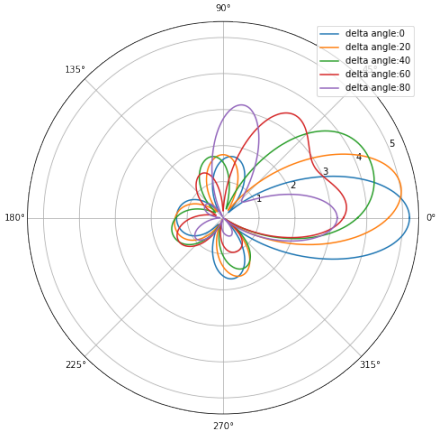

Figure 9. *Flexibeam* with two user clusters.

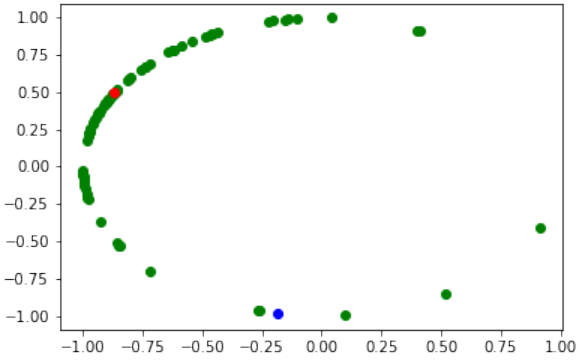

Figure 10. Simulated user distribution.

fact that under the same condition, *flexibeam* could increase throughput by propagating signals to more users.

Overall, both of these two methods perform well in our simulations. For *flexibeam*, the radiation area expands with the growing number of antennas and Θ. Besides, it can target several directions simultaneously so that we don't need to implement TDMA like what we do for matched beamforming.

B. Real data

In this part, we use two real datasets to evaluate the effectiveness of matched beamforming and *flexibeam*. For the sake of notation, we denote these two sets as dataset-I and dataset-II.

Users' accurate coordinates and covariance matrix of signal strength are given in dataset-I and dataset-II. The datasets contains 10000 signal covariance matrices for a duration of 10 seconds. In dataset I, the BS with 19 antennas

lies in the origin, and these antennas are evenly distributed on a circle of radius $r = \lambda = 0.3368\,\mathrm{m}$. 121 users locate in three clusters, with DOA in range 0, $(80°, 101°)$, and $(181°, 274°)$ respectively.

We estimate DOA by the Capon's beamforming. Fig 11 shows the derived power in all directions in the first time slot. The green dots in the figure correspond to the real sources, i.e., users. It can be seen that three peaks lie in the range of these users, which are regarded as the desired DOA. Thus, it shows that our DOA estimation is relatively accurate and these results can be used to apply beamforming algorithms later.

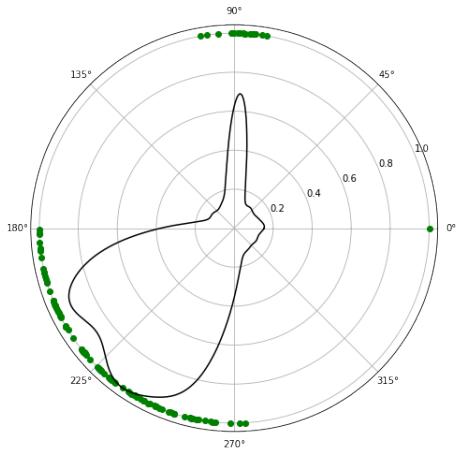

Figure 11. Power in all directions and real sources.

Because we use TDMA in matched beamforming, signal is pointed to one direction at a time. Fig. 12 plots the radiation pattern formed by matched beamforming in the first time slot of dataset-I. The radiation pattern focuses on one direction.

Then, we apply *flexibeam* on this dataset. Based on the DOA estimation, the radiation pattern of *flexibeam* is demonstrated in Fig. 13. From the plot, we can see that *flexibeam* generates two lobes with high power pointing to two user clusters as expected, but the radiation power in other directions is also relatively high, e.g. the transmitting power near 135° is also very high. This causes some waste on the transmitting energy since actually no user lies in that area. Besides, the beamwidth of these two main lobes is still small, and cannot cover a wide range of users. This phenomenon is mainly from the fact that all antennas have the same distance away from the origin, so the performance of *flexibeam* boils down to matched beamforming.

In terms of dataset-II, the number of antennas in this dataset is 15, and their position changes to rectangles with different radii (i.e., different distances to the origin). The antenna structure is shown in Fig. 14.

Matched beamforming's performance in dataset-II is acceptable and meets our expectation. As shown in Fig. 15, in the first time slot the main lobe radiates to direction 231° with other directions annihilated. But obviously, *flexibeam* generates more main lobes with larger beamwidths in this dataset, and Fig. 16 illustrates its radiation pattern in the first second.

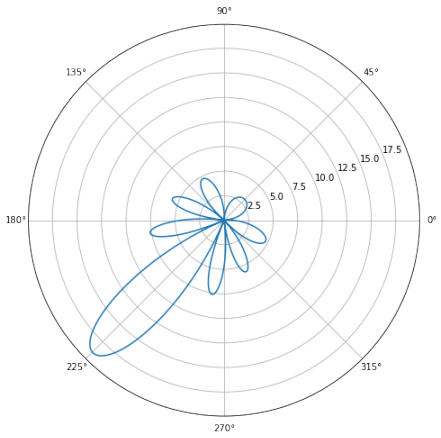

Figure 12. Radiation pattern generated via matched beamforming with dataset-I.

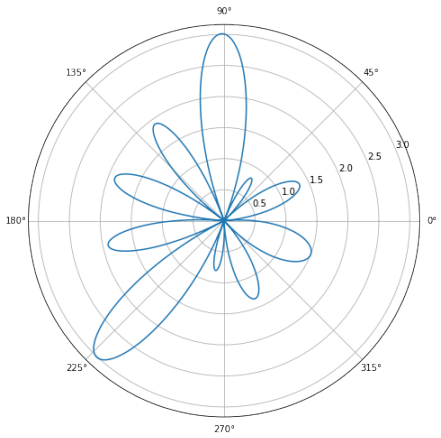

Figure 13. Radiation pattern generated via *flexibeam* with dataset-I.

Compared to the results of dataset-I, dataset-II has a wider radiation area. This is because antennas' radii are different, which indicates how closely the beamforming achieves the target radiation filter over the 2D area depends strongly on the number and position of the antennas.

Finally, we calculate the data rate with these datasets.

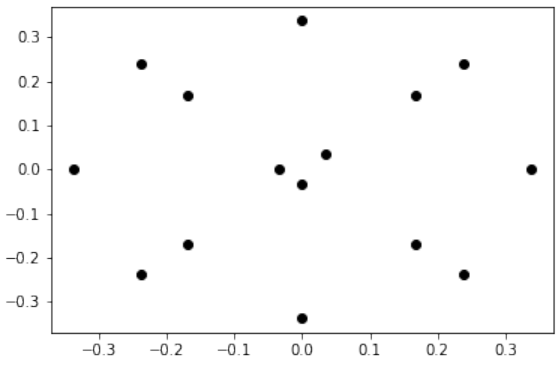

Figure 14. Antenna geometry in dataset-II.

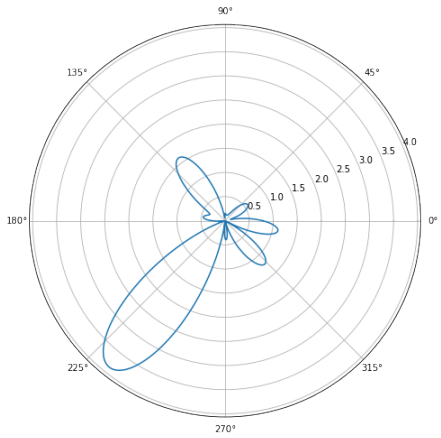

Figure 15. Radiation pattern generated via matched beamforming with dataset-II.

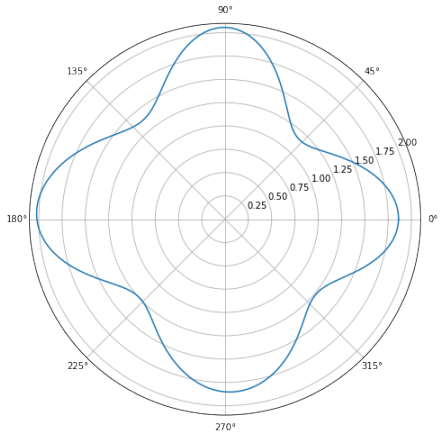

Figure 16. Radiation pattern generated via *flexibeam* with dataset-II.

Table II summarizes the average throughput with these datasets. The main factor leading to the increment in dataset-I is that *flexibeam* forms different main lobes to connect to different clusters simultaneously rather than using TDMA. A greater difference occurs in dataset-II, because all antennas' distances away from the origin vary compared with dataset-I. Thus, under this condition *flexibeam* can form a wider beam than matched beamforming and cover more users.

Table II
AVERAGE DATA RATE AMONG ALL USERS.

Dataset	Matched (bps)	*Flexibeam* (bps)	Improvements
Simulation	8.31×10^4	1.34×10^5	61.25%
dataset-I	4.31×10^4	5.73×10^4	32.95%
dataset-II	4.35×10^4	5.91×10^4	35.86%

IV. Discussion and Conclusions

In this project, we explore how to use matched beamforming and *flexibeam* to optimize the average throughput in a cellular network system. We first derive the mathematical expressions of these two algorithms. Then, we numerically calculate the radiation pattern and average throughput under different conditions with simulated and real data. Based on these numerical results, we analyze both algorithms' advantages and disadvantages.

When users slowly move in a limited area or all users distribute in dense, i.e, the estimated DOA is close to the real DOA, matched beamforming has a really good performance, leading to a really high data rate for all users. However, as long as users lie scattered or the DOA estimation is inaccurate, the throughput will decrease dramatically. This strict requirement makes it almost impossible to be applied in real scenarios. *Flexibeam* can form multiple main lobes with different beamwidths, so that it can cover a wide range of area, and is more robust to small user density and estimation errors of DOA than matched beamforming. However, to acquire a good performance, the base station is supposed to have a large number of antennas that are in a specific geometry, otherwise the average throughput would degrade. Thus this algorithm is suitable for real implementations when these requirements on the system infrastructure are satisfied.

V. Future Works

In this project, the system model is a relatively simple one. We do not consider many factors which actually affect the performance of these algorithms, like MIMO, channel fading, handover, and so on. So in future works, implementing a more complex and more general system model and making modifications to these algorithms based on the model would be a meaningful topic. Besides, errors in channel coding, channel estimation can be quantified in a more precise way, which can lead to a better evaluation about algorithms in real scenarios.

REFERENCES

[1] M. Agiwal, A. Roy, and N. Saxena, "Next generation 5g wireless networks: A comprehensive survey," *IEEE Communications Surveys Tutorials*, vol. 18, no. 3, pp. 1617–1655, 2016.

[2] F. Sohrabi and W. Yu, "Hybrid digital and analog beamforming design for large-scale antenna arrays," *CoRR*, vol. abs/1601.06814, 2016. [Online]. Available: http://arxiv.org/abs/1601.06814

[3] W. Roh, J.-Y. Seol, J. Park, B. Lee, J. Lee, Y. Kim, J. Cho, K. Cheun, and F. Aryanfar, "Millimeter-wave beamforming as an enabling technology for 5g cellular communications: theoretical feasibility and prototype results," *IEEE Communications Magazine*, vol. 52, no. 2, pp. 106–113, 2014.

[4] P. Hurley and M. Simeoni, "Flexibeam: Analytic spatial filtering by beamforming," in *2016 IEEE International Conference on Acoustics, Speech and Signal Processing (ICASSP)*, 2016, pp. 2877–2880.

[5] ——, "Beamforming towards regions of interest for multi-site mobile networks," in *International Zurich Seminar on Communications-Proceedings*. ETH Zurich, 2016, pp. 94–98.

[6] H. Krim and M. Viberg, "Two decades of array signal processing research: the parametric approach," *IEEE Signal Processing Magazine*, vol. 13, no. 4, pp. 67–94, 1996.